Proceedings of the AIAA 8th Applied Aerodynamics Conference, Portland, OR. AIAA 90-3073
August 20 - 22, 1990.

AERODYNAMIC SHAPE OPTIMIZATION OF HYPERSONIC MISSILES

George S. Dulikravich[1], Robert N. Buss[2],
Eric J. Strang[3], Seungsoo Lee[4]
Department of Aerospace Engineering
The Pennsylvania State University
University Park, PA 16802, U. S. A.

ABSTRACT

For bodies at zero incidence in hypersonic flow, the minimization of pressure drag was investigated. Using Modified Newtonian Theory (MNT), a general analytical model and a numerical optimization algorithm were developed for bodies comprised of cross-sections determined by the super-elliptic Lame function. This function enables the modeling of circular and elliptical cross-section bodies along with bodies whose cross-sections vary from a "star" to a "square". MNT accounts for pressure drag on body surfaces directly exposed to the free stream so that the coefficient of pressure drag is strictly a function of body geometry and the stagnation pressure coefficient. Using MNT, a computer code was written to minimize the normalized pressure drag by changing the body shape. The body volume and length were fixed in accordance with an initial input shape. The computer code then varied the super-elliptic Lame function parameters along the length of the body in a search for a minimum value of the normalized pressure drag. This was performed for three different classes of bodies. The results of the test cases compared well with linearized known analytic solutions for the optimum ogive shapes.

INTRODUCTION

The objective of this investigation is to demonstrate the feasibility of a hypersonic missile shape optimization method for minimizing the pressure drag. A computer code was used that employs MNT in order to analyze the pressure drag of a body in Mach 8+ flow which cannot be analyzed by conventional means. MNT states that for those surfaces which are exposed to the oncoming flow, the local pressure coefficients are given by multiplying the stagnation pressure coefficient at the nose tip by the cosine of the angle between the outward normal to the surface and the oncoming flow squared.

Previous work in the field of optimization of missile bodies in hypersonic flow [1,2,3,4,5] addressed the case where the geometry of the missile is axisymmetric. In contrast, this paper extends optimization to the cases where the radial coordinate of the missile is a function of the angular coordinate. We decided to represent the hypersonic missile cross-sections by utilizing the super-elliptic Lame function where the cross-section radial coordinate vary as a function of three parameters: a, b, and n. Our tests allowed for : (1) all circular cross-sections (a=b, n=2), (2) all elliptical cross-sections (a≠b, n=2), (3) Lame cross-sections with all three parameters a, b, and n independently varying, and (4) Lame cross-sections with only n varying.

When deriving an analytical expression for the pressure drag, the following assumptions were made: (1) the body has two planes of symmetry, (2) the body is slender lengthwise, (3) free stream angle of attack is zero, (4) the base plane is perpendicular to both planes of symmetry, (5) the freestream flow is parallel to both planes of symmetry and thus perpendicular to the base plane, (6) the base drag is neglected, (7) the pressure coefficient is determined according to MNT, (8) the length is kept constant, and (9) the volume is kept constant during the drag minimazation.

PRESSURE DRAG

The optimization code employs an analytical expression for the pressure drag. The pressure drag is a function of the missile body geometry and the nose tip stagnation coefficient of pressure. MNT for hypersonic flow was used to determine this expression. A Cartesian coordinate system was used to describe the missile body geometry (Fig. 1). The missile body has cross-sections based on the super-elliptic Lame function. This function consists of three geometric parameters; a, b and n. The function is given as

$$\left(\frac{x}{a}\right)^n + \left(\frac{y}{b}\right)^n = 1 \qquad (1)$$

Clearly, if a=b and n=2 then the above function describes a circle. As n --> ∞, the shape approaches a square. When n=1 the shape becomes a rhombus, and when n<1 the shape becomes "starred" (Fig. 2).

The super-elliptic function can be manipulated into polar coordinates as follows:

$$x = R\cos\theta$$
$$y = R\sin\theta \qquad (2)$$

where (R,θ) is the local polar coordinate system of a crosss-section. Hence,

$$R = \frac{ab}{[(a\sin\theta)^n + (b\cos\theta)^n]^{1/n}} \qquad (3)$$

[1]Associate Professor, Senior Member AIAA.

[2]Undergraduate Assistant, Student Member AIAA. Presently with GE, Evandale, OH.

[3]Undergraduate Assistant, Student Member AIAA. Presently graduate student at MIT, Boston, MA.

[4]Postdoctoral Fellow, Member AIAA.

The analytical expression for pressure drag was developed using the MNT for hypersonic flow. This theory states that for those surfaces on the missile body that are exposed to the flow, the local pressure coefficient, C_p, is given as:

$$C_p = C_{p_o} \cos^2\beta_n \tag{4}$$

where C_{p_o} is the stagnation coefficient of pressure and β_n is the local surface normal angle. This equation can be restated as:

$$C_p = C_{p_o} \sin^2\beta_t \tag{5}$$

where β_t is the local surface tangential angle.

Under the assumption that the body is slender, and that the radius is a function of θ and z, the pressure coefficient becomes [6]:

$$C_p = \frac{C_{p_o} R^2 R_z^2}{R^2 + R_\theta^2} \tag{6}$$

Given the length of the missile ,L, the drag is defined [7] as:

$$D = \int_0^L \left\{ \int_0^{2\pi} R \, \Delta P \, R_z d\theta \right\} dz \tag{7}$$

After dividing this expression with the dynamic pressure of the free stream, q_∞, and since, $C_p = \Delta P / q_\infty$, the analytic expression for the normalized pressure drag becomes [8]:

$$\frac{D}{C_{p_o} q_\infty} = \int_0^L \left\{ \int_0^{2\pi} \frac{R^3 R_z^3}{R^2 + R_\theta^2} d\theta \right\} dz \tag{8}$$

The radius, defined in equation (3), must be differentiated with respect to θ and z so that:

$$\frac{dR}{d\theta} = - \frac{ab}{[A + B]^{1/n+1}} \left[A \frac{\cos\theta}{\sin\theta} - B \frac{\sin\theta}{\cos\theta} \right] \tag{9}$$

where

$$A = (a \sin\theta)^n \quad ; \quad B = (b \cos\theta)^n. \tag{10}$$

Since $R = R(a,b,n)$, R_z becomes:

$$R_z = \frac{dR}{dz} = \frac{dR}{da}\frac{da}{dz} + \frac{dR}{db}\frac{db}{dz} + \frac{dR}{dn}\frac{dn}{dz} \tag{11}$$

where

$$\frac{dR}{da} = \frac{bB}{[A + B]^{1/n+1}} \tag{12}$$

$$\frac{dR}{db} = \frac{aA}{[A + B]^{1/n+1}} \tag{13}$$

$$\frac{dR}{dn} = \frac{R}{n^2} \left[\ln(A + B) - \frac{A \ln A + B \ln B}{A + B} \right] \tag{14}$$

The final expression for the normalized pressure drag can be obtained by substituting equations (3) and (9)-(14) into equation (8).

OPTIMIZATION OF MISSILE GEOMETRY

After an equation for $D/C_{p_o}q_\infty$ has been developed for a missile in hypersonic flow, it would be desirable to find the missile geometry which minimizes this quantity. In order to do this, several steps must be performed. First, the missile body is assigned an initial configuration. From this shape, its volume and $D/C_{p_o}q_\infty$ are determined. Next, the missile body is slightly changed while maintaining a constant volume. A new $D/C_{p_o}q_\infty$ is calculated for the changed shape. This is done for several body changes whereupon the shape having the minimum $D/C_{p_o}q_\infty$ is chosen as a new initial shape. The global iteration cycle, using a Q-P gradient search optimization algorithm [9], is repeated until a certain tolerance between cousecutive changes in the Lame function parameters a, b, and n is met.

The initial missile shape is defined by N cross-sections, including the nose (i=1) and the base (i=N). Each section is assigned separate values for the Lame parameters a, b, and n. A linear variation of these parameters is used between adjacent sections. Given these section parameters, each cross section area is determined by

$$S_i = 2\Delta\theta \left(\tfrac{1}{2} r_1^2 + r_2^2 + r_3^2 + \ldots + r_{k-1}^2 + \tfrac{1}{2} r_k^2 \right) \tag{15}$$

where

$r_1 = r(\theta = 0)$
$r_2 = r(\theta = \Delta\theta)$
$r_3 = r(\theta = 2\Delta\theta)$, $0 \le \theta \le \pi / 2$
$r_i = r(\theta = (i-1)\Delta\theta)$
$r_k = r(\theta = \pi / 2)$

Using the cross-sectional areas, the total volume is determined from

$$Vol = \sum_{i=1}^{N-1} \frac{(S_i + S_{i+1})}{2} (z_{i+1} - z_i) \tag{16}$$

This volume will be held constant throughout the optimization of the missile geometry, thus constituting a global constraint. Next, $D/C_{p_o}q_\infty$, is calculated for the initial missile configuration. In order to determine $D/C_{p_o}q_\infty$, the mid-point sectional parameters of the Lame function are represented as:

$$a_m = \frac{a_{i+1}+a_i}{2} \qquad b_m = \frac{b_{i+1}+b_i}{2} \qquad n_m = \frac{n_{i+1}+n_i}{2} \tag{17}$$

The axial derivatives from equation (11) for each set of adjacent cross-sections are represented as:

$$\frac{da}{dz} = \frac{a_{i+1} - a_i}{z_{i+1} - z_i}, \frac{db}{dz} = \frac{b_{i+1} - b_i}{z_{i+1} - z_i}, \frac{dn}{dz} = \frac{n_{i+1} - n_i}{z_{i+1} - z_i} \tag{18}$$

Integrating with respect to θ from 0 to $\pi/2$ for a set of cross-sections, $(D/C_{p_o}q_\infty)/dz$ for the entire cross-section is determined from

$$\frac{(D/C_{p_o}q_\infty)}{dz} = 4(\tfrac{1}{2} f_1 + f_2 + f_3 + ... + f_{k-1} + \tfrac{1}{2} f_k) \tag{19}$$

where

$$f_k = \frac{R^3 R_z^3}{R^2 + R_\theta^2} \tag{20}$$

Then $(D/C_{p_o}q_\infty)_i$ is

$$(D/C_{p_o}q_\infty)_i = \frac{(D/C_{p_o}q_\infty)}{dz} (z_{i+1} - z_i) \tag{21}$$

Finally, the normalized pressure drag for the initial missile configuration is:

$$\frac{D}{C_{p_o}q_\infty} = \sum_{i=1}^{N-1} (\frac{D}{C_{p_o}q_\infty})_i \tag{22}$$

A decrease in $D/C_{p_o}q_\infty$ is sought by changing the initial missile shape. For a given cross section, each Lame function parameter is decreased by a certain percentage factor, F. The necessary change at another cross section is then determined in order to maintain a constant missile volume. At this point, the $D/C_{p_o}q_\infty$ is found for the changed body. Afterwards, the $D/C_{p_o}q_\infty$ for each cross section with respect to every other axial section are calculated for each section parameter a, b, and n. Then the body with the greatest decrease in $D/C_{p_o}q_\infty$ is chosen as the new missile configuration and the procedure is repeated. In the event that a decrease has not been found, F is halved and then the procedure is repeated using the old missile body instead of a new shape. If F becomes less than a specified minimum percentage factor, F_{min}, the missile body with a minimum pressure drag has been found for the specified initial volume.

RESULTS

The initial configuration of the missile shape used in the first three test cases is depicted in Fig. 3 and will be referred to as shape A. The initial missile shape used in the fourth test case is depicted in Fig. 9 and will be refered to as shape B. The initial missile shape used in the fifth test case is depicted in Fig. 13 and will be referred to as shape C. The shapes were divided into 21 cross-sections and each cross-section was divided into 76 angular sub-sections. The initial missile shapes A and B had a non-dimensional volume of 0.0105. Shape A had a normalized pressure drag $D/C_{p_o}q_\infty$ = 0.000314. The convergence criterion used in these cases was: $F_{min} \leq 10^{-5}$.

In the first test case, all missile cross-sections were represented by circles (a=b, n=2). The optimized missile shape can be seen in Fig. 4. For the first 40 iterations, $D/C_{p_o}q_\infty$ decreased rapidly as can be seen in Fig. 5. After 40 $D/C_{p_o}q_\infty$ decreased rapidly as can be seen in Fig. 5. After 40 iterations, drag reductions were very small and $D/C_{p_o}q_\infty$ eventually became 0.000170 after 364 iterations. This represents a 46% reduction from the initial drag.

In the second test case, the allowed cross-sections had varying axes ($a \neq b$, n=2). For the first 10 iterations, $D/C_{p_o}q_\infty$ decreased rapidly and then leveled out (Fig. 6). The optimization code terminated after 314 iterations giving the same shape as the one given in test case 1 (Fig. 4). The final $D/C_{p_o}q_\infty$ was .000163 representing a reduction from the initial drag of 48 %.

In the third test case, the entire Lame function was allowed to vary ($a \neq b$, $n \neq$ const) for each cross-section. Even though all three parameters were allowed to vary simultaneously, $D/C_{p_o}q_\infty$ decreased in the same manner as in test case 2. After iteration 311, the optimization code terminated with a $D/C_{p_o}q_\infty$ of .000163 giving a reduction of 48 % of the initial drag.

Two analytical solutions for optimum ogive shapes have been used in order to determine the validity and accuracy of the shape optimization code. The results from the axisymmetric case were used for comparison. The first comparison was made with the shapes obtained from power law solutions (Fig. 7). The plot consists of a 3/4 - power body curve, a 2/3 - power body curve, the initial shape curve and the optimized body curve. The second comparison was made to the Sears - Haack [10] body for minimum drag and the von Karman ogive for minimum drag (Fig. 8). The optimized shape was found to fall between the von Karman ogive and the Sears-Haack body.

In the fourth test case, a star-shaped initial missile shape was used (Fig. 9). Allowing only the parameter n to vary, $D/C_{p_o}q_\infty$ decreased extremely rapidly in the first 6 iterations (Fig. 10) and extremely slowly thereafter requiring 6600 iterations to approach, but not reach, the desired convergence of $F_{min} = 10^{-5}$. The optimization was manually terminated (due to time constraints) resulting in the shape shown in Figs. 11 and 12. The final $D/C_{p_o}q_\infty$ was .000248 giving a drag reduction of 39% from the initial normalized drag of .000407. Notice that the front end of the missile retained its "star" shape which has been proven experimentally [11] to have lower drag.

In the fifth test case, a blunt circular cylinder (Fig. 13) was optimized resulting in an already familiar ogive shape (Fig. 7 and Fig. 8). Here, all three Lame parameters

(a, b, n) were allowed to vary along the missile. The drag reduction amounted to 99.8%.

CONCLUSIONS

The presented shape optimization of missile bodies in hypersonic flow is a feasible method of minimizing pressure drag in preliminary design. In the class of shapes represented by circular cross-sections, our results compared favorably with theories such as Power Laws for hypersonic bodies, Sears-Haack body, and von Karman ogive. This proves that our optimization algorithm is accurate. In the class of shapes comprised of general elliptical cross-sections, the bodies converged to axisymmetric geometry. However, we had unusual results when the initial cross-sections were represented by the "star" shapes. Instead of converging to a body with circular cross-sections, the optimal missile shape began with a "starred" nose which gradually varied into round cross-sections which in turn varied into rounded square cross-sections at the base of the missile. In all test cases, the drag of the initial cylinder shape was reduced significantly.

Even though our optimization algorithm works quite well, it can still be greatly improved. For example, skin-friction drag and surface heat transfer can be added to the present analysis of pressure drag [12]. Incorporating modifications due to centrifugal force effects, frequently called Newtonian-Busemann theory [13], would be a trivial modification. Similarly, we highly recommend improving the optimization method itself since the present optimization algorithm is relatively time consuming, although it runs in a matter of minutes on a VAX type machine.

In addition, missiles with curved centerlines and fins could be optimized or generated using this approach.

ACKNOWLEDGEMENTS

The authors wish to extend their thanks and appreciation to Erik Simon, Keith McGinniss, Robert Kampia and Sven Olevall for their help with the graphics and typing. We would like to thank Apple Computer for the donated equipment used in this work.

REFERENCES

[1] Large, E., "Nose Shape for Minimum Drag in Hypersonic Flow", The Journal of the Aerospace Sciences, pp. 98-99, 1962

[2] Miele, A., "Lift-to-Drag Ratios of Slender Bodies at Hypersonic Speeds", The Journal of the Astronautical Sciences, Vol. xiii, No.1, pp. 1-6, 1966.

[3] Miele, A., and Huang, H. Y., "Lift-to-Drag Ratios of Lifting Bodies at Hypersonic Speeds", Rice University, Aero-Astronautics Report No. 29, 1967.

[4] Huang, H. Y., "Conical Bodies of Given Length and Volume Having Maximum Lift-to-Drag Ratio at Hypersonic Speeds, Part 2, Variational Methods", Rice University, Aero-Astronautics Report No. 36, 1967.

[5] Strand, T., "Design of Missile Bodies for Minimum Drag at Very High Speeds - Thickness Ratio, Lift, and Center of Pressure are Given", The Journal of the Aero/Space Sciences, pp. 568-70, 1959.

[6] Miele, A., Heideman, J.C., and Pritchard, R. E., "Conical Bodies of Given Length and Volume Having Maximum Lift-to-Drag Ratio at Hypersonic Speeds, Part 1, Direct Methods", Rice University, Aero-Astronautics Report No. 34, 1967.

[7] Cox, R. N.,"Elements of Hypersonic Flow", Academic Press, New York, London, 1965.

[8] Miele, A., "Similarity Laws for Bodies Maximizing the Lift-to-Drag Ratio at Hypersonic Speeds", The Journal of the Astronautical Sciences, Vol. xiii, No. 5, pp. 116-20, 1966.

[9] Pshenichny, B. N., "Numerical Methods in Extremal Problems," MIR Publishers, Moscow, 1969.

[10] Ashley, H. and Landahl, M., "Aerodynamics of Wings and Bodies", Addison Wesley Publishing Company, 1965.

[11] Gonor, A. L. and Shvets, A. I., "Study of the Shock System for Flow Past Star-Shaped Bodies," Fluid Dynamics Russian Research, 1966, pp. 65-67.

[12] Brown, S.L., "Axisymmetric Bodies of Minimum Drag in Hypersonic Flow", Texas Center for Research Report U-TEX-EMRL-TR-1016, July 1967.

[13] Eggers, A.J., Resknikoff, M.M., and Dennis, D.H., "Bodies of Revolution Having Minimum Drag at High Supersonic Aerospeeds", NACA Report 1306, 1957.

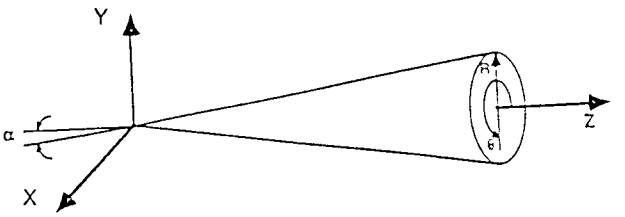

Figure 1: Description of coordinate system

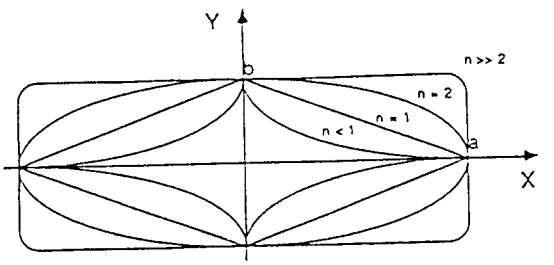

Figure 2: Super-elliptic functions: variation of exponent n

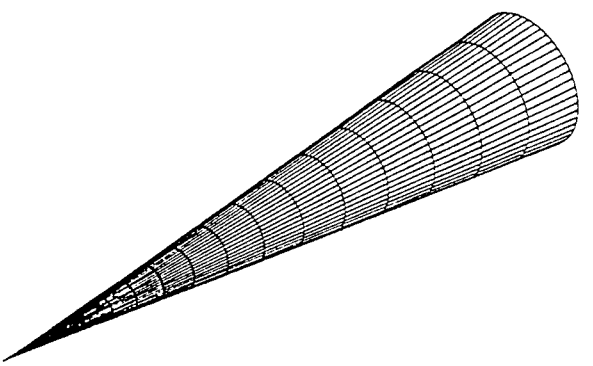

Figure 3: Initial configuration for first three test cases (shape A)

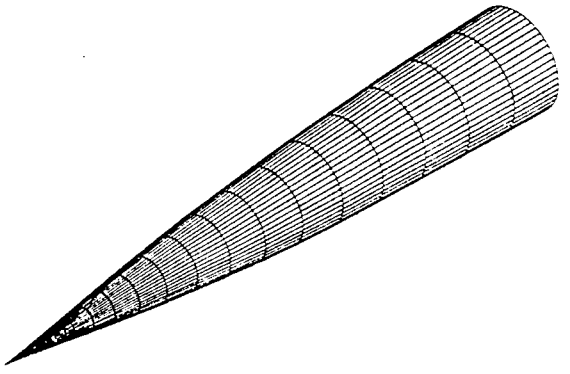

Figure 4: Optimized converged configuration for the initial shape A after 364 iterations (case 1), 314 iterations (case 2), and 311 iterations (case 3).

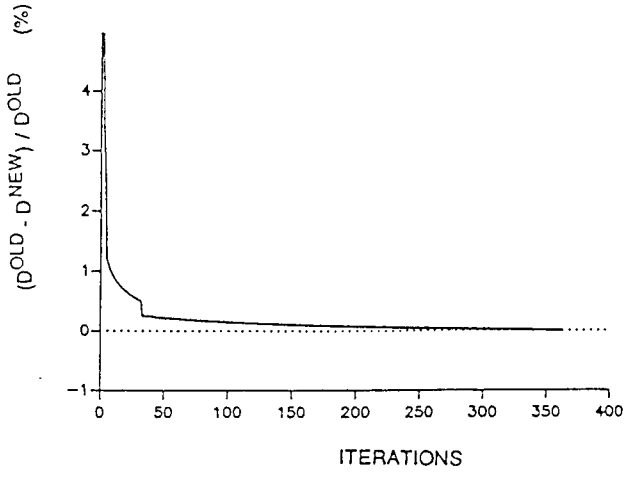

Figure 5: Test case no. 1: convergence history

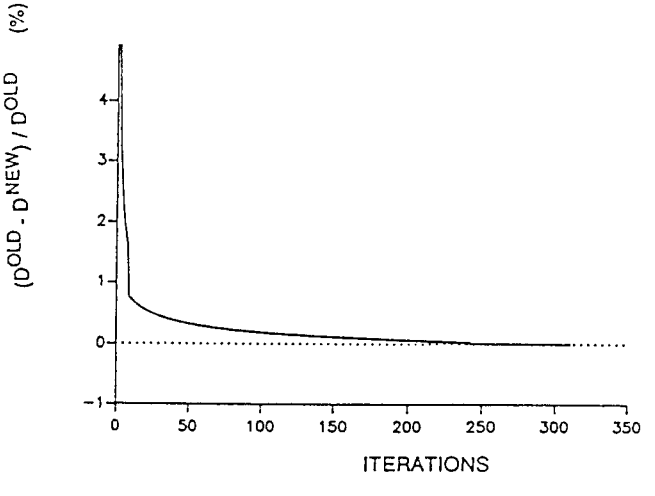

Figure 6: Test cases 2 and 3: similar convergence histories

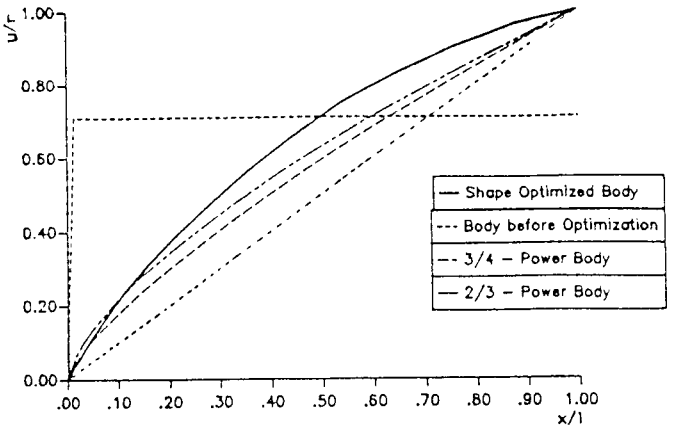

Figure 7: Comparison of optimized and power law hypersonic shapes

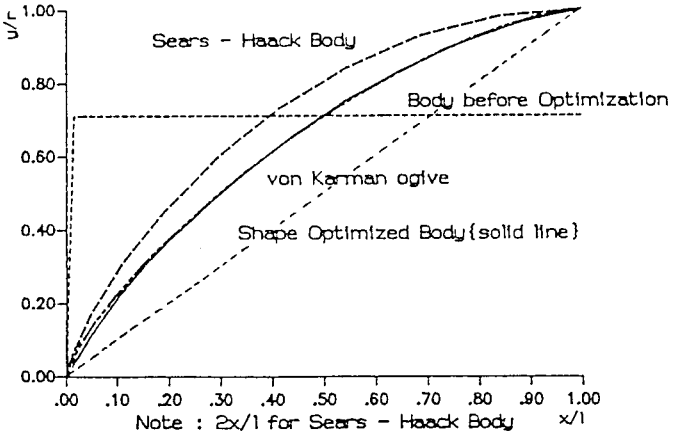

Figure 8: Comparison of optimized, von Karman and Sears-Haack optimum body shape

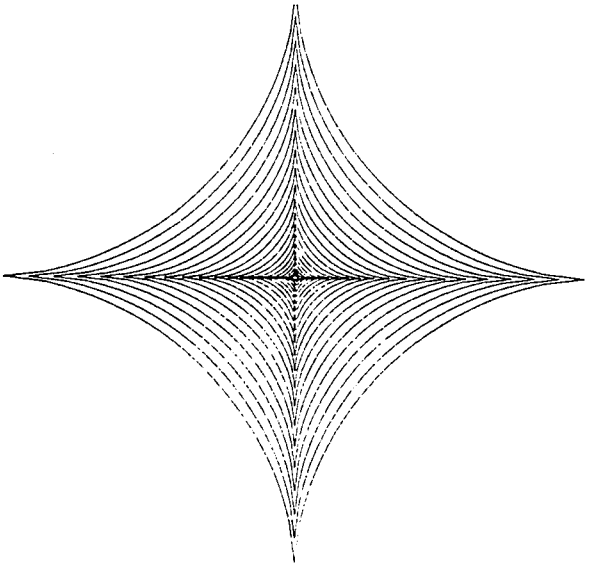

Figure 9: Test case 4: front view of the initial configuration (shape B)

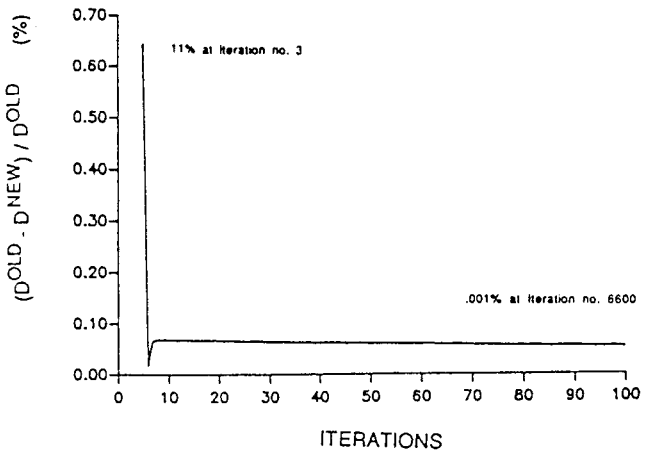

Figure 10: Test case 4: convergence history

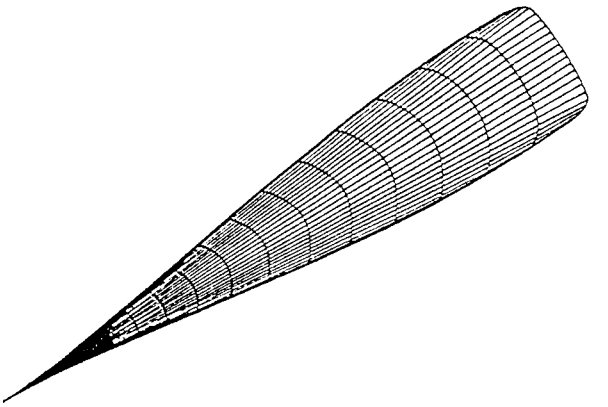

Figure 12: Test case 4: Optimized configuration after 6600 iterations (shape B)

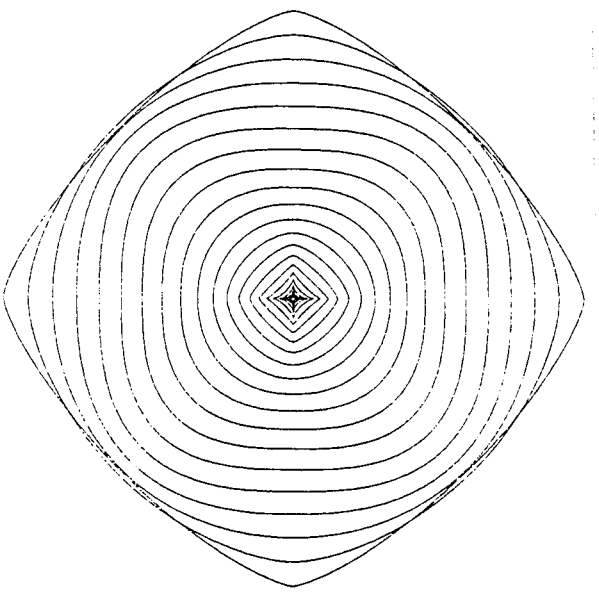

Figure 11: Test case 4: front view of optimized configuration (shape B)

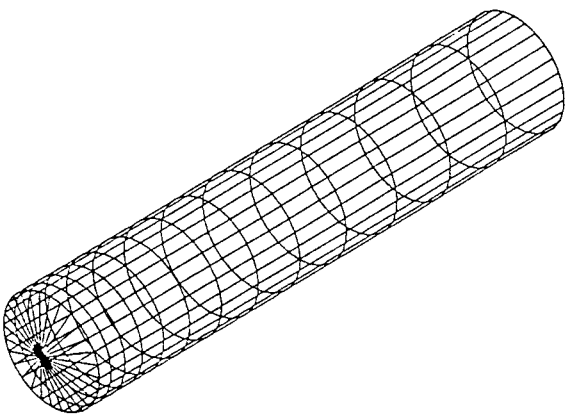

Figure 13: Test case 5: initial configuration (shape C)